



Microstructural Characterization of Polycrystalline Si Films Grown by Vapor-Induced Crystallization of Amorphous Si Using Al/Ni Chloride

Ji Hye Eom, Kye Ung Lee, and Byung Tae Ahn^{*,z}

Department of Materials Science and Engineering, Korea Advanced Institute of Science and Technology, 373-1 Guseong-dong, Yuseong-gu, Daejeon 305-701, Korea

A polycrystalline Si film with uniform and large grains can be grown by crystallizing with Al/Ni chloride vapor transport. At the initial stage of crystallization, the poly-Si grains had round-shaped cores with needles at the growth front. It showed that the needles were grown by the Ni-induced lateral crystallization process and the sidewall of the needles was enlarged by the Al-induced crystallization process. The needles were emerged coherently to an extent by the sidewall growth. As a result, a poly-Si film with grains larger than 15 μm diam and fewer intragrain defects was obtained. The Ni concentration was constant through out the film thickness with a value of $1 \times 10^{19} \text{ cm}^{-3}$. The Al concentration at the surface was 10^{19} cm^{-3} and was reduced below 10^{16} cm^{-3} at 25-nm depth. The thin film transistor utilizing the film showed an electron mobility of $47 \text{ cm}^2/\text{V s}$ at a drain voltage of $V_d = 0.1$. But the threshold voltage was 5.2 V that is considered as relatively high due to Al doping.
© 2007 The Electrochemical Society. [DOI: 10.1149/1.2429047] All rights reserved.

Manuscript submitted February 14, 2006; revised manuscript received November 6, 2006.
Available electronically January 18, 2007.

Demand for high-quality polycrystalline Si (poly-Si) thin films is increasing for applications involving the fabrication of electron devices such as thin-film transistors (TFTs) for organic light emitted diodes (OLEDs) and liquid crystal display (LCD), as well as for static random access memory (SRAM), electrically erasable and programmable read-only memory (EEPROM), and image sensors. In poly-Si films, grain boundaries, and microstructural defects within the grains degrade the performance of electron devices. Therefore, it is important to improve the quality of poly-Si films by reducing the number of intragrain defects and decreasing the size of the boundaries, which can be achieved by enlarging the area of grains. Many methods have been developed to improve the crystal quality in poly-Si films. The solid phase crystallization (SPC) of amorphous Si (a-Si) results in larger grains than direct deposition, but because the crystallization process involves twin formation, the resulting poly-Si grains contain many intra-grain defects.¹

Metal-induced lateral crystallization (MILC) using Ni metal is considered as one of the most effective and superior methods in SPC process.²⁻⁶ In the process, NiSi_2 precipitates are formed by Ni/Si chemical reaction and a needle grain is grown by the diffusion of Si from a-Si to crystalline Si through the precipitate. In the Ni MILC process, the direction of the needle grains is similar and a bundle of needle grains (quasi-grains) is created.⁷ However, this process is problematic as the bundle of needle grains consists of many low-angle grain boundaries and the poly-Si crystallized by the MILC process contains metal silicide residue.

Unlike Ni MILC, Al/a-Si system forms an amorphous mixing layer at the Al/Si interface. No Al-Si compound exists. In the Al-induced crystallization (AIC) process a crystalline Si grain is grown by the diffusion of Si through the Al/a-Si mixing layer and disk-shaped large grains are grown because a grain grows in the radial direction.⁸ In the process, Al remains in the crystalline Si film and acts as a shallow acceptor with the ionization energy of 67 meV, resulting in a p-type film.⁹ Because the ionization energy of Al is so small, the Al in the film does not act as a deep-level metal contaminant. Unfortunately, the poly-Si film grown by the direct Al/Si contact shows very rough surface and many voids.¹⁰

To improve the surface roughness in AIC process, vapor-induced crystallization (VIC) process using Al chloride has been introduced.¹¹ Recently, utilizing Al/Ni chloride vapor greatly lowered the crystallization temperature down to 480°C and the grain size was increased above $15 \mu\text{m}$.¹² The final poly-Si film had very

smooth surfaces due to 20 nm thick surface oxide that prohibits the extrusion of poly-Si crystallites at the film surface.

The growth mechanism of large grains by the Al/Ni chloride VIC process is not fully understood and the electrical property of the TFT using the poly-Si film crystallized is not known yet. In this study, we investigated the microstructure of the poly-Si film crystallized by the VIC process and fabricated TFTs using the film. It was found that the microstructure of the poly-Si film was greatly improved by the synergy effect of the Ni MILC process and AIC process.

Experimental

100 nm thick a-Si films were deposited on oxidized Si wafers at 550°C using SiH_4 by low-pressure chemical vapor deposition. The a-Si films were crystallized in an annealing furnace by the Al/Ni chloride VIC process.¹² The source for VIC was composed of $\text{AlCl}_3:\text{NiCl}_2 = 10:1$ and was transported from the source zone as a vapor phase by Ar flow to the annealing zone with a-Si film. Ar was continuously supplied before and during the annealing. To investigate the initial stage of crystallization, the annealing was conducted at 480°C for 1 h.

The microstructure of the poly-Si film was observed using optical microscopy (OM), scanning electron microscopy (SEM), and transmission electron microscopy (TEM). For SEM grain boundary observation, the remaining a-Si was removed by Secco etching with a solution consisting of $\text{CrO}_3:49\% \text{HF}:\text{H}_2\text{O} = 0.75 \text{ M}:1:100$.

N-channel TFTs with the poly-Si were fabricated. For the gate oxide, a 100 nm thick SiO_2 layer was deposited by inductively coupled plasma (ICP) chemical vapor deposition. Magnetron sputtered Mo was used for the gate metal. The source/drain regions were ion-shower doped with phosphorous plasma at room temperature with a 5 kV acceleration voltage and activated at 600°C for 1 h. No offset structure was used in the TFTs. A 300 nm thick SiO_2 was deposited by plasma enhanced chemical vapor deposition (PECVD) as an interlayer insulator. After contact-hole opening, a 500 nm thick Al was deposited by sputtering. The sample was annealed at 450°C for 30 min in $10\% \text{H}_2/\text{N}_2$.

Results and Discussion

Figure 1a shows the OM image of fully crystallized poly-Si grains grown on a-Si film annealed at 480°C for 10 h in an Al/Ni chloride vapor. The grains are impinged together and show various octagonal disk shapes. The grain size is about $15 \mu\text{m}$ and is very uniform. Figure 1b shows a higher magnification SEM image of a poly-Si grain core grown in the a-Si film annealed at 480°C for 1 h

* Electrochemical Society Active Member.

^z E-mail: btahn@kaist.ac.kr

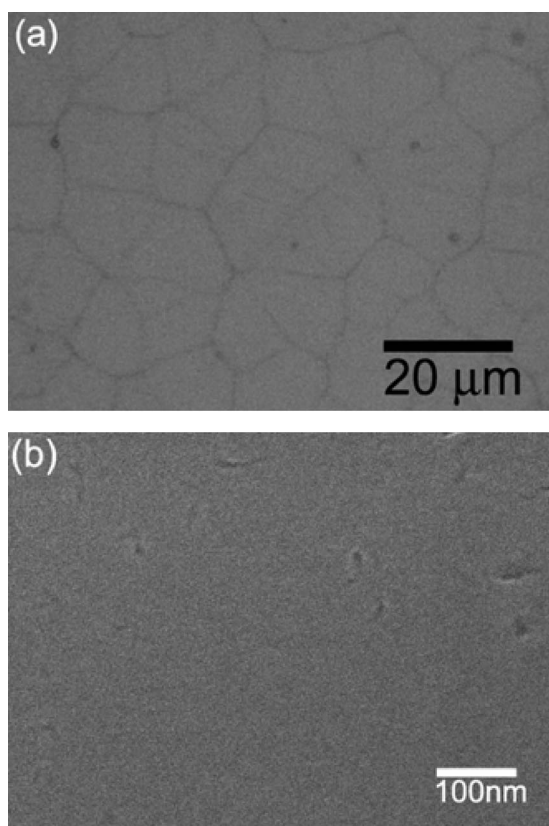


Figure 1. (a) OM image of Al/Ni chloride crystallized Si film and (b) SEM of Al/Ni chloride VIC poly-Si grain core.

in an Al/Ni chloride vapor. The core of the grain shows a dense and smooth surface. No significant inherent structural defects were observed.

Figure 2 shows the SEM image of initial stage poly-Si grains grown on a-Si film using various MIC methods. Figure 2a shows the initial stage grains grown by Ni MIC using Ni solution, annealed at 550°C for 1 h. The needle grains are distributed randomly all over the films.⁶ Figure 2b shows the initial stage grains by AlCl₃ VIC, annealed at 550°C for 5 h. The grains had a round-shaped growth front. The needle grains are formed in Ni MIC process, while the round-shaped grains are grown in Al MIC process.¹² Figure 2c shows the initial stage grains by Al/Ni chloride VIC, annealed at 480°C for 1 h. The poly-Si grains had round-shaped cores with needles at the growth front. In the Al/Ni chloride VIC process, the grains are of a completely different shape than in the either Ni or Al MIC process. Figure 2d shows the magnified growth front of a grain shown in Fig. 2c, which consists of a bundle of needles. These needles are well aligned in the same direction, indicating that the Ni MILC process takes place at the growth front. The growth direction by the Ni MILC process is $\langle 111 \rangle$ and the needles are either parallel or form 70° or 110° angles to one another.⁷ This alignment along the $\langle 111 \rangle$ direction is a critical factor for achieving large grains. However, the needles cannot merge in the Ni-MILC process because no NiSi₂ exists on the side of the needles. The NiSi₂ precipitates exist only at the tip of the needles. But in our Al/Ni chloride VIC process, the merge of two parallel needle grains are possible by side growth as seen in the next two figures.

Figure 3a shows the cross sectional TEM image of the needles at the growth front of the poly-Si grains, annealed at 480°C for 1 h in an Al/Ni chloride vapor. The needles (marked by arrows) are grown by Ni-MILC process and the long axis is outward of the paper.⁶ The cross section of the needles shows a triangular shape. For more

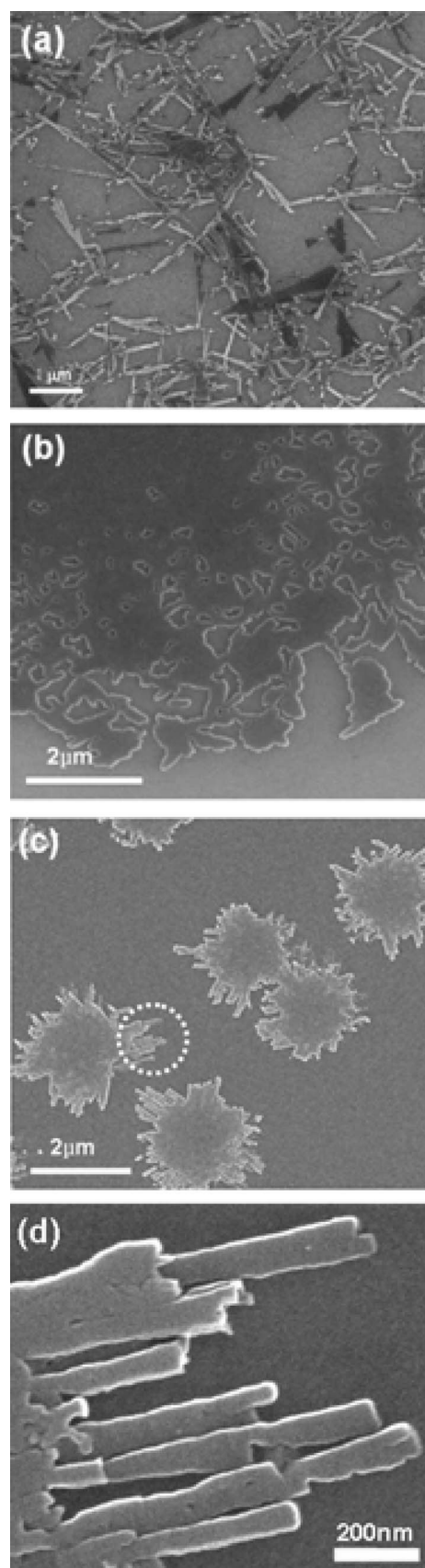


Figure 2. SEMs of crystallite grains in the Si films with various crystallization methods: (a) annealed at 550°C for 1 h by Ni solution MILC, (b) annealed at 550°C for 5 h by AlCl₃ VIC, (c) annealed at 480°C for 1 h by Al/Ni chloride VIC, and (d) magnified view of needles in Fig. 2c at the growth front.

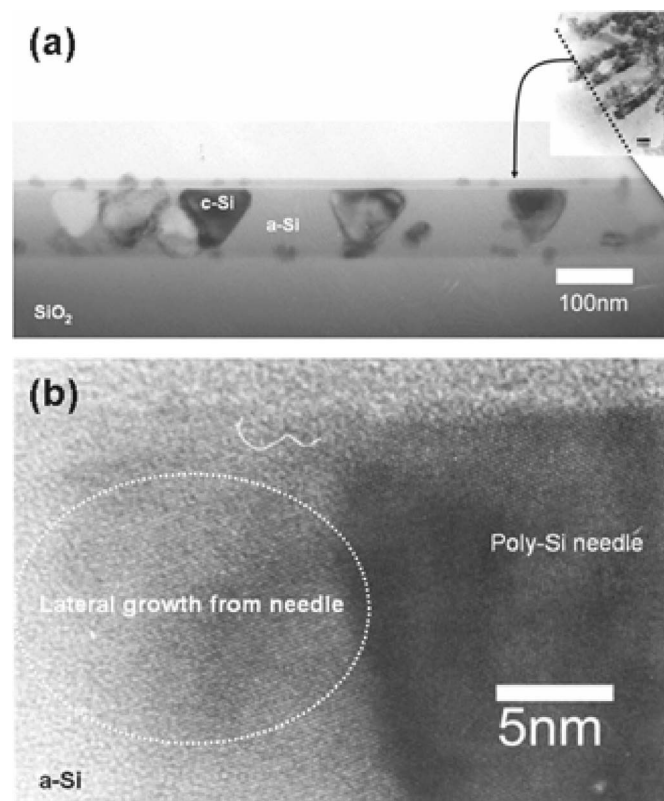


Figure 3. (a) Cross-sectional TEMs of Si film annealed at 480°C for 1 h by Al/Ni chloride VIC and (b) high-resolution TEM of the sidewall of a needle.

detailed characterization, high resolution TEM (HRTEM) observation was conducted on the triangular-shaped cross-section.

Figure 3b shows the HRTEM image near one of the needles. The dark area is the cross section of a needle. At the left side of the needle, a crystallized area can be seen and is grown from the sidewall of the needle. This sidewall crystallization is not possible in the Ni MIC process because no silicide exists on the sidewall of needle. It can be said, then, that the AIC process makes the side growth of needles grown by Ni-MILC possible. In other words, the width of needles increases with the help of AIC process.

Figure 4 shows a top view HRTEM image of a region where two needles are merged (dot circle). It shows two adjacent needles grown in the same direction, as discussed in Fig. 3, and a merged

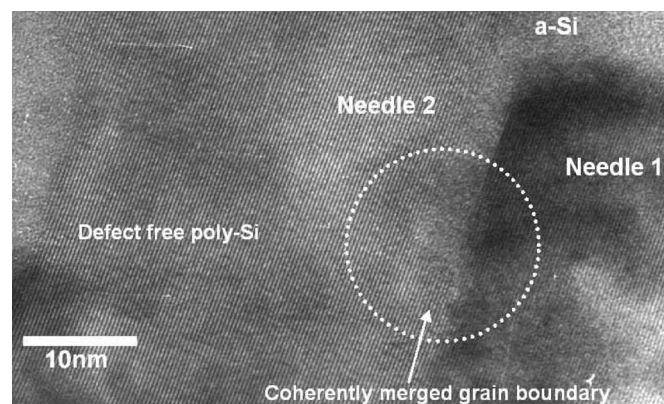


Figure 4. Plane-view high-resolution TEM of the interface where two needles merge in the poly-Si film crystallized at 480°C for 1 h by Al/Ni chloride VIC. The two needles merge nearly coherently.

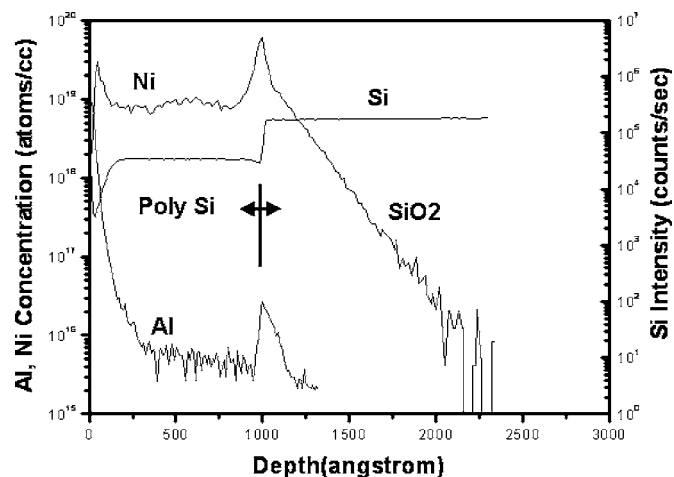


Figure 5. SIMS depth profile of Ni and Al concentrations in the poly-Si film crystallized at 480°C for 10 h by Al/Ni chloride.

interface with the help of AIC process. The interface between the merged needles is coherent and they become one grain. Because the needle itself is defect-free and the needles are merged coherently to a degree, the resultant grain can have much smaller number defects.

This process is repeated among other neighbor needles, resulting in very large grains with fewer defects within the grain. As a result of having fewer defects and large grains, the crystalline quality of poly-Si film is expected to be much improved.

One of the concerns using the Al/Ni chloride VIC process is metal contamination in poly-Si film and its effect on the performance of TFTs. Figure 5 shows a SIMS profile of Ni and Al concentrations in the crystallized Si film by the Al/Ni VIC process. The Ni concentration in the film was constant throughout the film with a value of 10^{19} cm^{-3} . Sohn et al. also reported that a large grain can be grown using a 100 nm thick SiN_x interlayer in Ni-MILC process and the Ni concentration in the film is 10^{19} cm^{-3} .^{13,14} On the other hand, the Al concentration is high up to 10^{19} cm^{-3} at the surface and it rapidly decreases. The Al concentration is dropped below

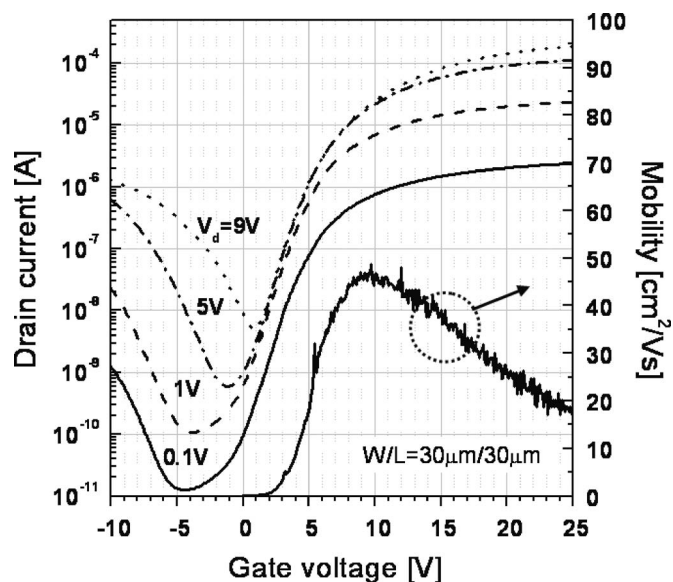


Figure 6. Drain current and field-effect mobility versus gate voltage for poly-Si TFTs employing a poly-Si channel crystallized by Al/Ni chloride VIC.

Table I. Device parameters of n-channel poly-Si TFT employing the poly-Si film crystallized by Al/Ni chloride VIC.

Parameter	V_D	
Threshold voltage (V_{th})	5.2 V	1 V
Field effect mobility (μ_{FE})	$47 \pm 2 \text{ cm}^2/\text{V s}$	0.1 V
Subthreshold slope	1.45 V/dec.	5 V
Minimum leakage current	$6.024 \times 10^{-11} \text{ A}$	5 V
On/off current ratio	1.9×10^5	5 V

10^{16} cm^{-3} at the depth of about 25 nm. Because the Al is a p-type donor, it is expected that the threshold voltage in TFT increases.

Figure 6 shows the drain current, I_D , as a function of the gate voltage, V_G , of the TFT fabricated using the VIC poly-Si film. The width and length of the TFTs are 30 and 30 μm , respectively. The threshold voltage is 5.2 V which is determined by the linear extrapolation of the maximum I_D/V_G slope in the I_D - V_G plot to the x-axis at $V_D = 0.1 \text{ V}$. The maximum field-effect mobility is $47 \pm 2 \text{ cm}^2/\text{V s}$, measured at $V_D = 0.1$. The subthreshold slope and on/off current ratio obtained from the transfer curve at drain voltage $V_d = 5 \text{ V}$ are 1.45 V/dec and 1.9×10^5 , respectively. The minimum leakage current is $6 \times 10^{-10} \text{ A}$ at $V_d = 5 \text{ V}$, which should be further reduced by improving source/drain junction. The device parameter of n-channel poly-Si TFT is summarized in Table I.

The threshold voltage of 5.2 V is considered as a slightly high compared to 1-2 V in the conventional Ni-MILC process.³ Threshold voltage is linearly proportional to the gate-oxide thickness so that it can be reduced with a thinner gate oxide. The mobility value is considered as comparable to that of Ni-MILC process where the mobility is in the range of $40 \text{ cm}^2/\text{V s}$.^{15,16} However, the mobility value is not large enough considering the large grain size and low structural defect within the grains. One of the possible reasons is that surface Al doping that is ionized and acts as a scattering center. The threshold voltage can be reduced and the mobility can be further increased by reducing the Al concentration at the film surface. The Al doping might be reduced if the film surface is consumed by plasma oxidation or by growing an additional thin intrinsic Si layer that is under current study.

However, the existence of a small amount of Al might be useful to obtain a reliable and uniform threshold voltage through out the large area display panel. Because our grain size is large enough to fabricate a single-grain TFT if the TFT size is small, the individual grain might be used for TFTs. In the case the TFT does not contains grain boundaries so that the mobility of individual TFTs might be

much higher. It is very interesting to develop a single-grain TFT because of higher mobility and better reproducibility and is beyond the scope of this paper.

Conclusions

The microstructures of poly-Si films crystallized by Al/Ni chloride VIC process were investigated. The poly-Si grains showed round-shaped cores with needles at the growth front. The needles at the growth front were grown by Ni MILC process and the sidewall of the needles grew and merged with the help of AIC process. Because the needles were aligned in specific directions by MILC process the interface between the merging needles was coherent to a considerable extent. As a result, a poly-Si film with grains larger than 15 μm with fewer intragrain defects was successfully grown. The Ni concentration was constant through out the film thickness with a value of $1 \times 10^{19} \text{ cm}^{-3}$. The Al concentration decreases rapidly with the values of 10^{19} cm^{-3} at the surface and below 10^{16} cm^{-3} at the 25 nm depth. The thin film transistor utilizing the film showed the threshold voltage of 5.2 V and electron mobility of $47 \text{ cm}^2/\text{V s}$ at a drain voltage of $V_d = 0.1 \text{ V}$. The threshold voltage was high and the mobility was not high enough due to Al doping and the doping effect could be reduced with a thinner gate oxide and with surface oxidation during TFT fabrication.

The Korea Advanced Institute of Science and Technology assisted in meeting the publication costs of this article.

References

1. J. H. Kim, J. Y. Lee, and K. S. Nam, *J. Appl. Phys.*, **77**, 1 (1995).
2. D. K. Sohn, S. C. Park, S. W. Kang, and B. T. Ahn, *J. Electrochem. Soc.*, **144**, 3592 (1997).
3. S. W. Lee and S. K. Joo, *IEEE Electron Device Lett.*, **17**, 160 (1996).
4. J. Jang, J. Y. Oh, S. K. Kim, Y. J. Choi, S. Y. Yoon, and C. O. Kim, *Nature (London)*, **395**, 481 (1998).
5. S. I. Jun, Y. H. Yang, J. B. Lee, and D. K. Choi, *Appl. Phys. Lett.*, **75**, 2235 (1999).
6. J. H. Ahn and B. T. Ahn, *J. Electrochem. Soc.*, **148**, H115 (2001).
7. J. H. Ahn, J. H. Eom, and B. T. Ahn, *J. Electrochem. Soc.*, **151**, H141 (2004).
8. T. K. Konno and R. Sinclair, *Philos. Mag. B*, **66**, 749 (1992).
9. O. Nast, S. Brehme, D. H. Neuhaus, and S. R. Wenham, *IEEE Trans. Electron Devices*, **46**, 2062 (1999).
10. O. Nast and S. R. Wenham, *J. Appl. Phys.*, **88**, 124 (2000).
11. J. H. Ahn, J. H. Eom, and B. T. Ahn, *Sol. Energy Mater. Sol. Cells*, **74**, 315 (2002).
12. J. H. Eom, K. U. Lee, and B. T. Ahn, *Electrochem. Solid-State Lett.*, **8**, G65 (2005).
13. J. H. Choi, D. Y. Kim, B. K. Choo, W. S. Sohn, and J. Jang, *Electrochem. Solid-State Lett.*, **6**, G16 (2003).
14. W. S. Sohn, J. H. Choi, K. H. Kim, H. H. Oh, S. S. Kim, and J. Jang, *J. Appl. Phys.*, **94**, 4326 (2003).
15. J. B. Lee, D. K. Choi, and Y. H. Yang, *Thin Solid Films*, **408**, 240 (2002).
16. C. W. Chao, Y. C. S. Wu, G. R. Hu, and M. S. Feng, *Jpn. J. Appl. Phys., Part 1*, **42**, 1556 (2003).